Contents lists available at ScienceDirect

Environment International

Protein-affinity guided identification of chlorinated paraffin components as ubiquitous chemicals

Yibin Sun, Hongyang Cui, Tong Li, Shu Tao, Jianying Hu, Yi Wan[*]

Laboratory for Earth Surface Processes, College of Urban and Environmental Sciences, Peking University, Beijing 100871, China

ARTICLE INFO

ABSTRACT

Chlorinated paraffins (CPs) have been extensively examined to identify their components. Short-chain CPs with a carbon number of 10–13 have been strictly restricted or banned due to their addition to the list of Persistent Organic Pollutants in the world. However, more constituents with potential toxicities in these complicated mixtures are still unclear. In the present study, a purification method based on the protein affinity of thyroid hormone-related proteins (transthyretin and thyroid receptor) was established. The protein-based affinity extraction coupled with high-throughput scanning successfully discover a new group of chlorinated compounds ($CP(O_2)$) in commercial CP mixtures. The $CP(O_2)$s were purified from the commercial mixtures and identified to be chlorinated fatty acid methyl esters (CFAMEs) with a carbon chain length of 17–19 and 3–11 chlorines by a combination of liquid-liquid extraction, hydrolysis, Fourier transform infrared spectrometry and Orbitrap mass spectrometry. The newly identified CFAMEs were found to be ubiquitous in the environmental matrices, and concentration ratios of $\sum$CFAMEs/$\sum$CPs ranged from 0.01 to 35 in air, soil and food samples. CFAMEs were also detected in blood samples of general populations, and accumulated in humans through dietary uptake. CFAMEs can compete with T4 for binding TTR with higher potencies than CPs, possibly leading to disruptions of thyroid hormone homeostasis.

1. Introduction

Chlorinated paraffins (CPs) are high production volume chemicals and widely used in diverse applications including flame retardants, plasticizers, metal processing fluids and leather fat liquor, etc. (de Boer, 2010; Glüge et al., 2016b; Hahladakis et al., 2018; Henschler, 1994). These compounds are complicated mixtures of polychlorinated n-alkanes, and the well-known constituents include short-chain CPs (SCCPs; C10–13), medium-chain CPs (MCCPs; C14–17) and long-chain CPs (LCCPs; C $\geq$ 18) (de Boer, 2010). Although these three groups of CPs have been found to be ubiquitous and persistent in various environmental matrices (Gao et al., 2012; Harada et al., 2011; Houde et al., 2008; Tomy et al., 1999; van Mourik et al., 2015; Wang et al., 2013; Yuan et al., 2012; Zeng et al., 2013; Zeng et al., 2011), limited information is available on the toxic components of the mixtures (Ren et al., 2019; Wei et al., 2016). Current toxicity studies have mostly focused on SCCPs, and reported lethality (Bezchlebova et al., 2007; Bucher et al., 1987; Ren et al., 2018), hepatotoxicity (Cooley et al., 2001; Wang et al., 2019a; Wyatt et al., 1993), carcinogenicity (Bucher et al., 1987; Wang

et al., 2019a) and endocrine disruptions (Gong et al., 2018; Liu et al., 2016; Wyatt et al., 1993; Zhang et al., 2016) etc. Of these various toxicities, SCCPs can induce the disruption of thyroid hormones (THs) at a relatively low dose in rats (Gong et al., 2018; Wyatt et al., 1993), and these compounds were able to undergo placental transport and pose exposure risks to the fetus (Aamir et al., 2019; Chen et al., 2020; Qiao et al., 2018; Wang et al., 2018). Correspondingly, the use of SCCPs has been strictly restricted or banned in several nations including the United States, Japan, Canada, and Europe, and SCCPs were added to the list of Persistent Organic Pollutants (POPs) in the 2017 Stockholm Convention (UNEP, 2017; van Mourik et al., 2016). Therefore, identification of the toxic components of CP mixtures is vital for risk assessment and management of these compounds.

In contrast to limited toxicity studies of CPs, the widely used commercial CP mixtures are complex industrial products containing thousands of CP homologues (Feo et al., 2009), analogues (such as unsaturated CPs) (Li et al., 2018b; Schinkel et al., 2018), and even unknown components (Li et al., 2018b; Muir et al., 2000). Generally, the chlorine content and carbon chain length were specified for the

---

commercial mixtures by the manufacturers in Germany, the United Kingdom, the United States and China (Bogdal et al., 2015; Tomy et al., 1997). But the known CPs (SCCPs, MCCPs and LCCPs) are actually produced at low levels in the commercial mixtures (Li et al., 2018b; Xu et al., 2016). In the most commonly used CP-52 commercial mixtures, which accounts for 90% of the output in China (Glüge et al., 2016a; Tang and Yao, 2005), the mass fractions of SCCPs, MCCPs and LCCPs are only 0.6–17.5%, 13.0–21.4%, and 7.4–11.4%, respectively (Li et al., 2018b). Recently, the unsaturated CPs were identified, but their mass fractions were in the range of 1.9–11.8%, leaving approximately 36.8–60.8% of unknown components (Li et al., 2018b). To screen and identify the unknown toxic components in complex CP mixtures is challenging. Generally, environmental toxicological studies use toxicity identification-evaluation (TIE) or effect directed-analysis (EDA) to identify the key toxicants in complex mixtures in the environment (Ballesteros-Gomez and Rubio, 2011; Brack, 2003; Burgess et al., 2013b; Petrovic et al., 2004). However, these methodologies require multiple steps of sample fractionations and toxicity testing (Burgess et al., 2013a; Burgess et al., 2013b; Li et al., 2018a; Simon et al., 2015). In comparison, the purification method with protein affinity coupled with non-targeted screening by high-resolution spectrometry could directly identify the toxic compounds and their detailed structures (Hu et al., 2019; Peng et al., 2016; Ziegler et al., 2013). CPs, especially SCCPs and MCCPs, were reported to exhibit thyroid disruption effects at a relatively low dose (USEPA, 2015; Wang et al., 2019b), leading to the reduced free TH levels in rats and mice (Birtley et al., 1980; Bucher et al., 1987; Gong et al., 2018; Poon et al., 1995; Wyatt et al., 1993). The homeostasis of THs, mainly mediated by TR and TTR, is essential in vertebrate development processes (Ishihara et al., 2003; Mondal et al., 2016; Ortiga-Carvalho et al., 2014; Pleasure et al., 2017; Volkov et al., 2020). SCCPs and MCCPs could undergo placental transfer possibly mediated through TTR, a transport protein facilitating the placental transfer of hydrophobic pollutants in pregnant women (Aamir et al., 2019; Chen et al., 2016; Chen et al., 2020; Hamers et al., 2020; Qiao et al., 2018; Wan et al., 2010; Wang et al., 2018). Thus, CPs may bind the TH transport protein (transthyretin, TTR) and thyroid receptors (TRs), leading to the adverse effects on TH homeostasis and fetal development. We hypothesized that affinity purification with TTR and TR proteins could identify the toxic components in commercial CP mixtures, which could help discover more unknown dominant CP components in the environment.

In this study, a purification method based on the protein affinity of TTR/TR was established and used to extract the active components in commercial CP mixtures. The extracted compounds were then screened by high-resolution mass spectrometry, and a series of CP structural analogues were successfully found with high mass fractions. The detailed structures of the unknown compounds were identified by a combination of liquid-liquid extraction, hydrolysis, Fourier transform infrared spectrometry and Orbitrap mass spectrometry. The unknown CP structural analogues in the commercial CP mixtures were finally identified as chlorinated fatty acid methyl esters (CFAMEs) with carbon numbers of 17–19 and chlorine numbers of 3–11. The wide occurrence of these newly identified CFAMEs was also confirmed in human blood and various environmental samples including air, soil, and foods. To our knowledge, this is the first study to identify the chlorinated paraffin analogues containing oxygen atoms in the environment. CFAMEs could bind TTR with high affinities and accumulate in humans through multiple exposure routes, especially the consumption of plant-based foods. More studies are needed to determine the environmental occurrence and risk evaluation of CFAMEs in the future.

2. Material and methods

2.1. Preparation and purification of His-tagged TTR/TR fusion protein

The circular DNA (cDNA) encoding full-length human TTR and ligand-binding domain (LBD) of the human TR were first amplified, and the amplified TTR & TR-LBD cDNA were then subcloned into the prokaryotic expression vector pET-48b containing a His-Tag. The recombinant plasmid pET-48b-His-TTR and pET-48b-His-TR-LBD were then transformed into *Escherichia coli* (*E. coli*) DH5α-competent cells by heat shock transformation (the mixture was incubated on ice for 30 min, at 42 °C for 90 s, and then transferred to ice for 3 min). The expression plasmids of pET-48b-His-TTR and pET-48b-His-TR-LBD were then transfected into *E. coli* BL21 DE3 cells by heat shock transformation. The expression of pET-48b-His, pET-48b-His-TTR and pET-48b-His-TR-LBD were induced with 0.2 mM isopropyl β-$_D$-thiogalactoside at 20 °C for 18 h. The recombinant proteins were purified with a nickel-affinity column (Ni^{2+}-charged HiTrap chelating high-performance column from GE Healthcare), followed by a Hitrap desalting column (GE Healthcare) to remove imidazole. The expression of pET-48b-His-TTR and pET-48b-His-TR-LBD were detected by sodium dodecyl sulfate-polyacrylamide gel electrophoresis (SDS-PAGE) (Fig. S1) with 4% stacking and 15% resolving, and the gel was stained with Coomassie brilliant blue. Plastic tubes (Corning Centristar, Corning, NY) were used during protein preparation, purification and preservation.

2.2. Screening protein binding chemicals using protein-based affinity purification

Protein-based affinity purification and non-target analysis were carried out to identify TTR/TR binding chemicals in the commercial CP mixtures. 1 mL of 20 μM pET-48b-His, pET-48b-His-TTR and pET-48b-His-TR-LBD (n = 6) was spiked with 1 μL commercial CP mixtures (50 μg/mL) and incubated in 2-mL glass tubes at 4 °C for 1 h. After adding 500 μL of His-select nickel magnetic beads (Beaver Life Science) to each tube, the mixture was incubated for 2 h in a shaker at approximately 170 rpm at 4 °C. After removing the supernatant using a magnetic separator, the residues were washed more than 10 times with 1 mL buffer (0.1 M KCl, 5 mM MgCl$_2$ and 20 mM Tris-HCl; pH 7.5), and the TTR/TR protein was then eluted from the His-select nickel magnetic beads with 1 mL buffer (0.1 M KCl, 5 mM MgCl$_2$, 20 mM Tris-HCl, and 250 mM imidazole; pH 7.5). The elution step was performed in triplicate. The chemicals bound to the TTR/TR protein were transferred to another glass tubes and extracted by adding 50 μL formic acid and ethyl acetate (3 mL for three times), followed by shaking on a vortex mixer for 2 min and centrifuging at 4,000 rpm for 5 min. The extraction was performed in triplicate, and the extract was evaporated to almost dryness under a gentle stream of nitrogen gas, and dissolved in acetonitrile for UPLC-QTOF MS analysis. A negative control experiment was also performed using the same protocol with pET-48b-His protein instead of pET-48b-His-TTR and pET-48b-His-TR protein. The efficiency of the recombinant TTR/TR to affinity purify chemicals was confirmed using the positive TTR/TR ligand L-thyroxine (T4) at concentrations of 0.1, 10 and 50 ng/mL. The average percentage of affinity purified T4 of the spiked concentration in the pET-48b-His-TTR and pET-48b-His-TR protein were 92% and 90%, respectively, and the average percentage of affinity purified T4 of the spiked concentration in the control group was 13% (Fig. S1).

The chemical features were extracted from the acquired MS data sets of the affinity purified extraction, and peaks with intensity above 5,000 were selected and aligned with the settings of "RT window" = 0.2 min and "mass window" = 5 ppm. The data were then exported into SIMCA-P+ (ver. 12.0, Umetrics, Umea, Sweden) for multivariate statistical analysis including the principal component analysis (PCA) and the orthogonal partial least-squares discriminant analysis (OLDS-DA). The unsupervised PCA showed the overview of relationships among groups, and the supervised OPLS-DA helped to identify the exact chemical features that contributed to the difference between the His-tagged TTR/TR groups and the control group. Chemical features with a significantly high intensity from the His-tagged TTR/TR group compared to the control group (*p*-value < 0.05 with Student's *t*-test) were extracted for analysis. The formulas of the extracted chemical features were

calculated with the following element parameters settled: C 0–50, H 0–100, 35Cl 0–100, 37Cl 0–100, N 0–20, O 0–20, and S 0–20. Formulas with a mass tolerance lower than 5 ppm and reasonable isotope abundance between ^{35}Cl and ^{37}Cl were accepted.

2.3. Isolation of CP(O₂)s

Some CP(O₂)s were identified based on the protein-based affinity purification and non-target analysis. Preparative HPLC was performed to isolate the individual CP(O₂)s with a Shimadzu high performance liquid chromatography system (LC-20AT) equipped with a UV detector (SPD-20A), using an YMC C18 preparative column (5 μm particle size, 250 mm × 10 mm i.d.). 1 mL of commercial CP mixture (CP-42, CP-52 and CP-70) was dissolved in 10 mL *n*-hexane, and injected into the preparative LC system with a volume of 250 μL. Acetonitrile at a flow rate of 3 mL/min was used as the mobile phases. The fraction from 7.14 min to 7.40 min was collected. The purified fraction was determined UPLC-qTOF-MS to confirm the isolated compounds to be CP(O₂)s. Also, the isolated compounds were incubated with TTR proteins, and all the CP(O₂)s were affinity purified.

Liquid-liquid extraction was further performed to determine whether CP(O₂)s were ionic or covalent. In a glass vial, 1 mL of isolated CP(O₂)s was evaporated under a gentle stream of nitrogen, followed by the addition of 1 mL of 2 M NaOH solution. After sufficient shaking, the neutral compounds in the aqueous phase were extracted with 2 mL of *n*-hexane three times. The acidic compounds were changed to neutral compounds by the addition of 1 mL of 3 M HCl into the vial, and the organic phase was extracted with 2 mL of *n*-hexane three times. UPLC-qTOF-MS analysis was then performed to determine whether the CP (O₂)s were acidic or neutral.

2.4. Hydrolysis

Hydrolysis was carried out to identify the structures of CP(O₂)s. In a 4 mL glass vial, 1 mL of isolated CP(O₂)s was evaporated under a gentle stream of nitrogen, followed by the addition of 1 mL of 2 M methanolic NaOH solution. The hydrolysis reaction was carried out at 40 °C for 20 min. Neutral compounds in the solution were firstly extracted with 2 mL of *n*-hexane three times. Then, 1 mL of 3 M HCl was added to the solution, and the acidic compounds were extracted with 2 mL of *n*-hexane three times.

2.5. UPLC-qTOF-MS analysis

Analysis was carried out using an ACQUITY UPLC system equipped with a Xevo qTOF-MS using an API-ESI source. A Waters ACQUITY UPLC BEH C18 column (50 × 2.5 mm, s-1.7 μm) was used for separation. The column temperature was 40 °C, and the injection volume was 3 μL. The flow rate was 0.1 mL/min, and conditions for the gradient elution were as follows: 90% water(A) and 10% methanol (B) remained for the first minute, linearly decreased to 70% A at 1.5 min, linearly decreased to 40% A at 2 min, linearly decreased to 0% A at 4 min, then maintained at 100% B from 4 min to 8.5 min, linearly increased to 70% A at 9 min, linearly increased to 90% A at 10 min, maintained at 90% A and 10% B for 1 min before the next injection. DCM at a flow rate of 10 μL/min was introduced to the mobile phase between UPLC and the ion source via a syringe pump between 5.5 and 8.5 min.

The UPLC-qTOF-MS was operated in full-scan (*m/z* 250–1600 covering the mass rang of CPs, *m/z* 350–1450), negative ion mode at a resolution of 25,000 and a scan time of 1 s. The following parameters were used for analysis: capillary voltage, 2.5 kV; sampling cone voltage, 40 V; extraction cone voltage, 4 V; source temperature, 100 °C; desolvation temperature, 250 °C; cone gas flow rate, 50 L/h; desolvation gas flow rate: 600 L/h; the lockspray reference compound was LE (leucine-enkephalin, *m/z* 554.2615, negative ion mode) and the calibration compound was sodium formate.

2.6. Orbitrap MS analysis

To confirm the structure of the identified CP(O₂)s, high resolution mass spectrometry (Orbitrap MS, Thermo Fischer Scientific) was applied to the isolated and hydrolyzed fractions. Extracts were dissolved in acetonitrile with the addition of 10% DCM. The analytes were directly injected into the APCI-Orbitrap MS, which was operated in negative ion mode with a resolution of 140,000. The following parameters were used for analysis: spray voltage 2.6 kV; capillary temperature 150 °C; Aux gas: 1arb, 50 °C; sheath gas: 8arb; maximum IT: 250 ms; AGC target: 5e6.

2.7. FT-IR spectroscopy analysis

A Nicolet iS50 FTIR spectrometer (Thermo Scientific) was used to identify the functional groups of the isolated and hydrolyzed CP(O₂)s. Absorption spectra were recorded at 4000 cm^{-1} ~ 400 cm^{-1} at a resolution of 2 cm^{-1} with 256 averaging scans. Acetonitrile spectra were obtained for subtracting solvent contribution. All spectra were processed by OMNIC 9.3.32 software (Thermo Fisher).

3. Results and discussion

3.1. Screening the TTR/TR competition-binding compounds

As CPs mainly exhibit thyroid disruption activities, the chlorinated compounds may bind the TH transport protein (transthyretin, TTR) and thyroid receptors (TRs) with high affinities (Bytingsvik et al., 2013; Hallgren and Darnerud, 2002; Ishihara et al., 2003; Mondal et al., 2016; Ucán-Marín et al., 2010). The components with potential binding affinities with TTR and TR were identified in the commercial CP mixtures by the application of a His-tagged TTR/TR fusion protein affinity purification coupled with dichloromethane (DCM) enhanced ionization-UPLC-QTOF-MS screening. The commercial mixtures included CP-42 (42% chlorine, w/w), CP-52 (52% chlorine, w/w) and CP-70 (70% chlorine, w/w) purchased from major manufacturing companies in provinces with high production volume of CPs in China, and compositions of CPs in the commercial mixtures have been reported previously (Li et al., 2018b). A total of 3,327 chemical features were detected by the non-target screening in the TTR, TR and control groups, and unsupervised principal component analysis (PCA) was used to determine the differences between the three groups. The PCA successfully represented the variability as the first two principal components accounted for 71.1% of the variance. As shown in Fig. S4, the TR and control groups were relatively close, especially in the direction of the first principal component axis, whereas the TTR group was far away from the other two groups. The results indicated that the commercial CP mixtures contained TTR binding compounds, which could be affinity purified by the TTR fusion protein and exhibited significant differences compared to the control group. In comparison, TR binding compounds were not found in the CP mixtures, which is consistent with the previous report that limited structural diversity was found for direct ligand effects on TR, and only 11 compounds directly interacted with TR among 8,305 chemicals in the Tox21 Chemical Library (Paul-Friedman et al., 2019).

Supervised orthogonal partial least-squares discriminant analysis (OPLS-DA) was further conducted to identify the key protein binding compounds that led to the class distinction in the TTR and control groups. The OPLS-DA plots showed that the TTR group was clearly separated from the control group at the predictive component axis (Fig. 1a). The model showed reliable predictive ability where the R2X (cum), R2Y (cum) and Q2 (cum) were 0.843, 0.998, and 0.966, respectively. Chemical features of TTR binding compounds were selected from S-plots constructed from the OPLS-DA analysis, and variables with significantly high intensity from the TTR group compared to the control group were selected ($p < 0.05$). In the three commercial mixtures tested, totally 828 chemical features in the TTR group were
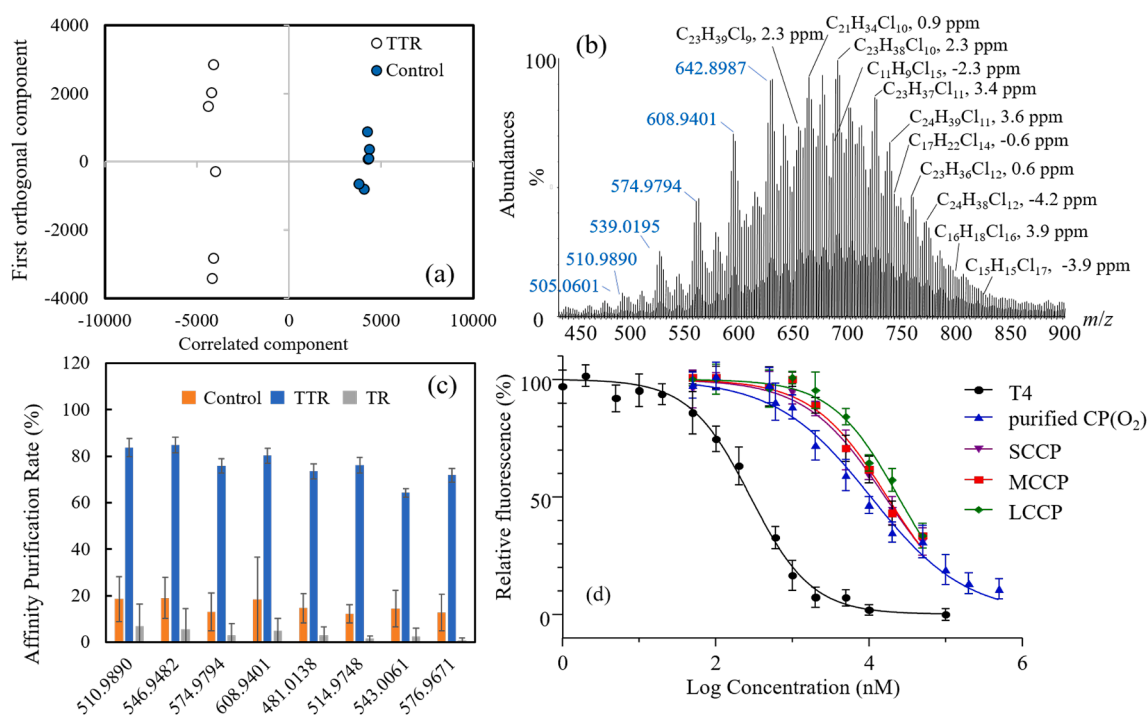
Fig. 1. a) OPLS-DA analysis of extracted chemical features from pET-48b-His-TTR and pET-48b-His (control) group. b) Mass spectra of chlorinated compounds extracted from a CP-70 commercial mixture by the TTR affinity purification, and CPs are marked in black and unknown components are marked in blue. c) Affinity purification rates of exemplified CPs and unknown components. d) Fluorescence displacement curve of CP(O₂), SCCP, MCCP and LCCP titrated into a solution of 0.6 μM ANSA and 0.5 μM TTR. Data represent the average of fluorescence intensity relative to an ANSA-TTR solution ± SD of at least three different experiments in triplicate. Lines represent the predicted values after the data were adjusted to a Hill model. (For interpretation of the references to color in this figure legend, the reader is referred to the web version of this article.)

extracted, and 476 features were identified to be chlorinated compounds based on the pattern of chlorine isotopic peaks. The MS spectra of the chlorinated compounds extracted from various commercial products are shown in Figs. 1b and S6. Among the TTR binding compounds, 99 CPs were identified including 22 SCCPs, 34 MCCPs, and 43 LCCPs according to their DCM enhanced ionization m/z ([M+Cl]⁻) and elemental composition (Table S3). The extracted compounds using the TTR protein affinity purification were affected by the abundances of the CP congener groups in the commercial mixtures and their binding affinities with TTR. For examples, numerous congeners of C_{17}-MCCPs and C_{24}-LCCPs were affinity purified and their corresponding high abundances were also reported in the commercial mixtures (Li et al., 2018b). The affinity purification rates (%) of CPs were calculated by comparing the abundances of each congener in the TTR protein affinity assays with those in the commercial mixtures (Fig. S5 and Table S3). And the TTR affinity purification rates of CPs ranged from 57.2% to 95.2%, which showed a similar value for CPs with carbon number of 10–15 and then a decreasing trend for $C_{>16}$-CPs. TTR has been proposed to be responsible for delivery of maternal thyroid hormones to the fetus (Landers et al., 2013; Patel et al., 2011), and some TTR-binding compounds, such as PCB, TBBPA, and PBP and PFAS, were shown to cross the placenta barrier due to TTR-mediated transport (Park et al., 2008; Weiss et al., 2009; Yang et al., 2016). Consistently, the observed TTR binding affinities of CPs in this study were similar to their placental transfer potentials between mother and fetus, in which the placental transfer efficiencies exhibited similar values for C_{10-14}-CPs, and then decreased with increasing carbon chain length for $C_{>15}$-CPs (Aamir et al., 2019; Chen et al., 2020).

Besides the known CP congeners, some chlorinated components affinity purified by the TTR protein contained two oxygen atoms based on the element analysis (57 chemical features), and have not been reported before (Table S3, Figs. 1b and S6). The TTR binding affinity of the unknown CP(O₂) compounds (70.0–92.7%) were higher than CPs with

similar carbon and chlorine numbers (62.5–89.8%). As shown in Fig. 1c, [M+Cl]⁻ ions with an m/z of 510.9890, 546.9482, 574.9794 and 608.9401 were shown to exemplify CP(O₂) compounds, m/z of 481.0138, 514.9748, 543.0061 and 576.9671 were selected to exemplify the CPs with similar carbon and chlorine numbers. These chlorinated compounds were recovered with high rates in the TTR group (63.5–88.8%), and low rates in the TR group (0.6–2.8%) and control group (8.1–18.1%). In addition, the binding affinities of CP(O₂)s and CPs to TTR were further confirmed by a previously reported ANSA(8-anilino-1-naphthalenesulfonic acid ammonium salt) displacement assay (Montaño et al., 2012; Zhao et al., 2017). As shown in Fig. 1d, CP(O₂)s and CPs showed specific TTR binding affinities, with 50% inhibition potency (IC₅₀) values of 10.5 ± 1.0 μM, 16.2 ± 1.4 μM, 17.3 ± 1.5 μM, and 24.2 ± 2.0 μM for purified CP(O₂)s, SCCPs, MCCPs, and LCCPs respectively, which were higher than 283 ± 19 nM for T_4. The IC₅₀ values also showed the binding affinity trends of CP(O₂)s > SCCPs > MCCPs > LCCPs, which was consistent with the affinity purification experiments. These results demonstrated that the unknown CP(O₂) compounds had stronger specific TTR-binding abilities compared to CPs, and these compounds had low affinity to the TR.

The unknown CP(O₂) compounds were suspected to contain functional groups such as OH (hydroxyl group), C—O—C (ether group), and C=O (carbonyl group) based on the element composition. A 3D plot of abundance, retention time (RT) and m/z of the TTR-binding compounds showed distinct peaks of CPs and CP(O₂) compounds (Fig. 2). The RTs of CP(O₂)s were around 6.52–6.89 min and those of CPs with similar carbon length were around 6.92–7.75 min (Fig. 2 and Table S3). The shorter RT indicated that the CP(O₂)s may be alcohols, ethers, aldehydes, ketones, acids, esters or other compounds that had relatively high polarity compared to CPs.
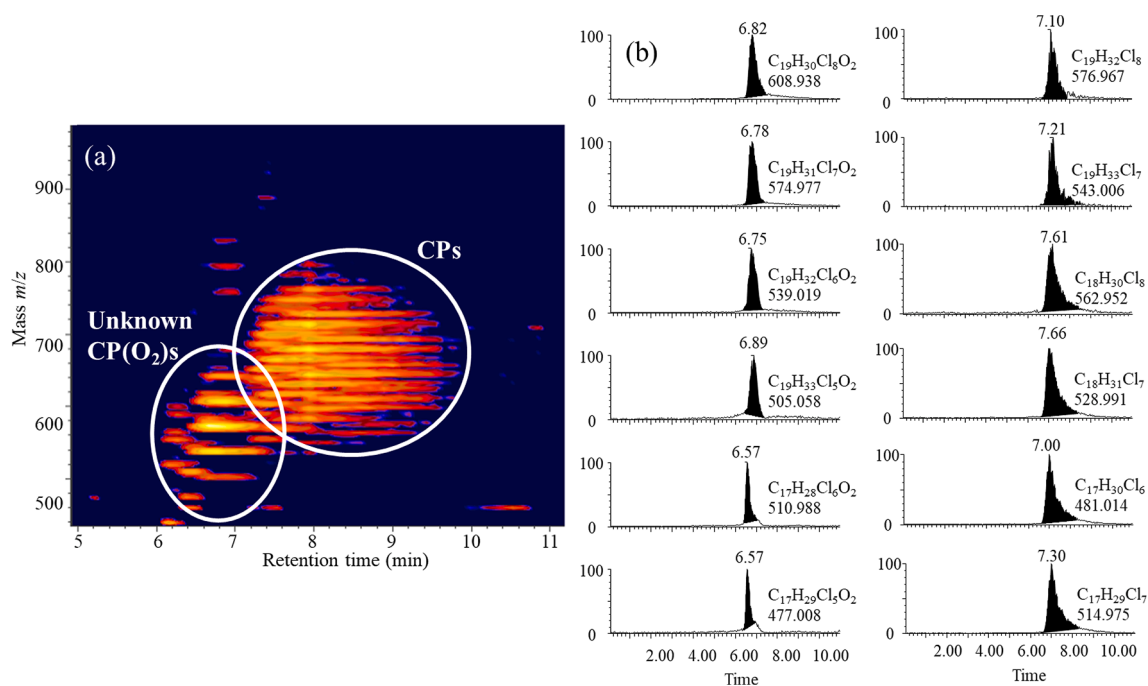
Fig. 2. a) Three-dimensional plot (retention time, m/z and abundance) of the chlorinated compounds using the affinity purification of the commercial CP mixtures. b) Chromatograph of the unknown CP(O$_2$)s and CPs with the same carbon and chlorine numbers.

3.2. Fractionation and hydrolysis of CP(O$_2$)s

The unknown CP(O$_2$) compounds were further isolated from the CP commercial mixtures by preparative chromatography for structure identification. The isolated CP(O$_2$)s were then treated with liquid-liquid extraction in different pH solutions. The CP(O$_2$)s were extracted from the solutions when the pH was adjusted to higher than 12 (Fig. 3a), and no compounds were subsequently found when the pH of solutions were acidified to less than 1 (Fig. 3b). These results indicated that CP(O$_2$)s were not ionized compounds such as alcohols or acids, and the two oxygen atoms in the compounds might be present in the form of an ester group, ether linkages or ketone groups.

Hydrolysis experiments were then carried out to identify the

functional group in the CP(O$_2$) compounds. As shown in Fig. 3c, CP(O$_2$)s were hydrolyzed under strong basic conditions, but no compounds were extracted from the basic solutions after hydrolysis, suggesting that CP (O$_2$)s did not contain functional groups of ether linkages or ketones. When the pH of the hydrolyzed solutions was adjusted to less than 1, a series of polychlorinated products with similar m/z profiles compared to the parent CP(O$_2$)s were extracted from the acidic solution (Fig. 3d). Of these hydrolyzed products, only the ions with low m/z including 393.0753, 429.0515, 455.0673 and 463.0127 were accurately identified based on element analysis. Two products (429.0515 and 463.0127) corresponded to the unhydrolyzed ions with m/z of 443.0673 and 477.0280 via the loss of CH_2, and the product of 455.0673 corresponded to ions of 505.0601 via the loss of CH_3Cl. High mass errors (-29.6 to
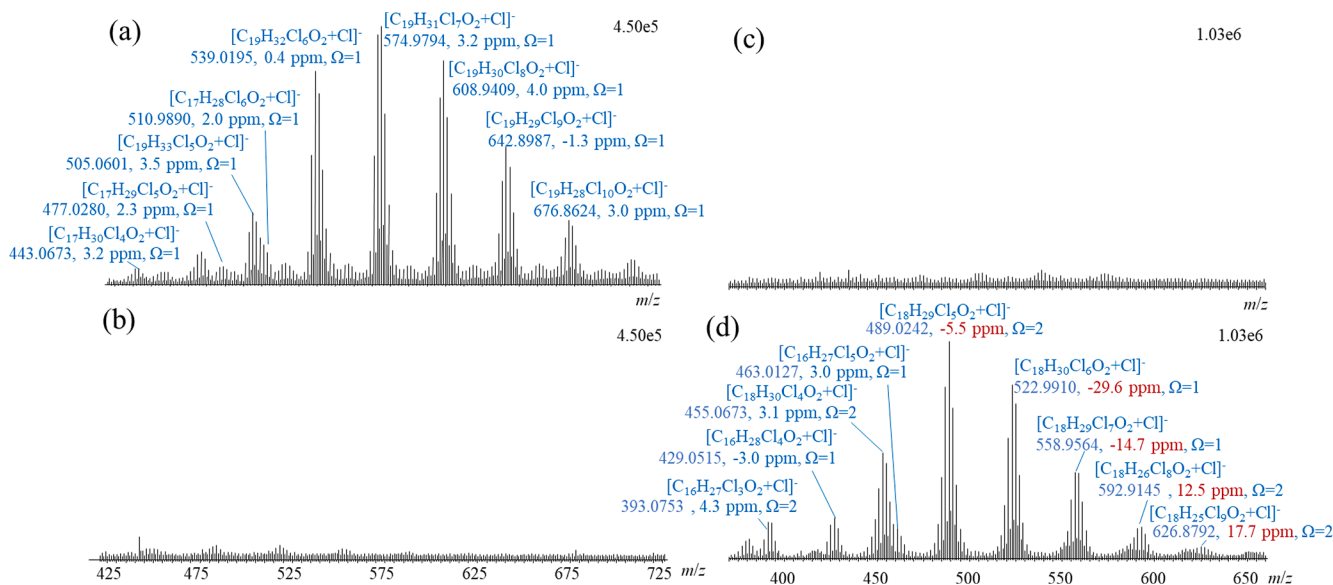
Fig. 3. Mass spectra of purified CP(O$_2$)s during liquid-liquid extraction: a) extracts in solution with pH > 12, b) extracts in solution when pH was changed to < 1. Mass spectra of hydrolysis products of purified CP(O$_2$)s extracted in solution with pH > 12 (c) and pH < 1 (d).

17.7 ppm) were observed for the ions with high m/z when they were matched with the most possible molecular formula, such as 522.9910, 626.8792, etc. It is interesting to note that all the identified products had various unsaturated degrees. Thus, it is possible that the CP(O$_2$)s could be esters and hydrolyzed to generate acids with an unsaturation degree (Ω) of 1 based on the cleavage of ester groups. In the hydrolysis solutions, the produced acids also underwent elimination reactions, leading to the generation of acids with higher unsaturation degrees ($\Omega > 1$) via the loss of HCl. The mixtures of acids with various unsaturation degrees made it difficult to accurately identify the ions with high m/z based on the QTOF-MS scanning with the resolution of 25,000. For example, the mass difference between [C$_{17}$H$_{28}$Cl$_5$COOH + Cl]$^-$ ($\Omega = 1$) and [C$_{17}$H$_{27}$Cl$_6$COOH-HCl + Cl]$^-$ ($\Omega = 2$) was 0.0186, and the separation of the two groups of ions required a mass resolution of R > 25,000 when the molecular weights of CPs were approximately 500. Thus, Orbitrap-MS with a resolution of 140,000 was performed to identify the compounds before and after hydrolysis.

The above hydrolysis studies generated a hypothesis that CP(O$_2$)s were possible esters. Fourier-transform infrared (FTIR) spectroscopy was carried out to verify the hypothesized structures of the unknown CP (O$_2$) compounds. Signals observed at 2960 ~ 2850, ~1460 and 737 cm^{-1} were assigned to C—H (sp^3, stretch), C—H (stretch), and C—Cl (stretch), respectively, which showed no significant changes after the hydrolysis reaction (Fig. 4). Characteristic signals at 1737 and 1300 ~ 1000 cm^{-1} were observed for CP(O$_2$)s before hydrolysis, and were assigned to C=O (stretch) and C—O—C (stretch), respectively, suggesting the presence of an ester group (Figs. 4 and S7). After the hydrolysis reaction, characteristic signals at 3200 ~ 2500 and 1709 with significant high abundance were observed, and were assigned to O—H (stretch, broad O—H bridges) and C=O (stretch), respectively, suggesting the presence of a —COOH group, which was further confirmed by signals at ~1380 and ~929 cm^{-1} for O—H (bend) (Figs. 4 and S7). Moreover, the lower frequency of C=O stretching than normal acid and the weak peak at 1683 cm^{-1} were found for the hydrolyzed products, which indicated that the presence of C=C may have been produced by side reactions (Figs. 4 and S7). Therefore, the unknown CP(O$_2$) compounds contained functional groups of esters based on the hydrolysis and FTIR analysis.

3.3. Structure identification of CP(O$_2$)s

During the hydrolysis reaction, some products with high unsaturation degrees were generated through the elimination reaction of

halogenated hydrocarbons as discussed above, leading to a strong mass interference under qTOF-MS analysis. To deal with these interferences, the compound mixtures before and after hydrolysis were directly injected into the DCM enhanced ionization-Orbitrap-MS with a resolution of 140,000 (Fig. 5). As shown in Fig. 5a, only CP(O$_2$)s (ester) were detected before hydrolysis and exemplified by C$_{19}$H$_{31}$Cl$_7$O$_2$, C$_{19}$H$_{32}$Cl$_6$O$_2$, and C$_{19}$H$_3$°Cl$_8$O$_2$, which were consistent with the results of QTOF analysis (Fig. 3a). Due to the extremely high resolution, more CP(O$_2$)s were detected with low abundances by qTOF-MS and were clearly observed by the Orbitrap-MS analysis, for example, C$_{17}$H$_{31}$Cl$_3$O$_2$, C$_{17}$H$_{30}$Cl$_4$O$_2$, and C$_{19}$H$_{34}$Cl$_4$O$_2$ as shown in Fig. 5a1, further demonstrating the presence of the CP structural analogues containing oxygen atoms.

After the hydrolysis reaction, the parent ions of esters all disappeared, and many groups of chlorinated compounds were generated in the extract of acidified solution. These compounds could not be identified in the element analysis using qTOF-MS, but mixtures of chlorinated acids with various unsaturation degrees were found, which were resolved by Orbitrap-MS. A serious of ions of the chlorinated acids with $\Omega = 1$ were detected (Fig. 5b). A one-to-one correspondence between the acids ($\Omega = 1$) and CP(O$_2$)s was found only based on the loss of CH$_2$. As shown in Fig. 5a and b, the one-to-one correspondence between the two sets of isotope clusters before and after hydrolysis is shown in the same color, for example, the green isotope clusters for C$_{19}$H$_{33}$Cl$_5$O$_2$ around 505.05940 and C$_{17}$H$_{30}$Cl$_5$COOH around 491.04339 were a reactant-product pair. The results indicated that CP(O$_2$)s were all methyl esters. Moreover, isotope clusters of acids with the higher degree of unsaturation ($\Omega > 2$) were also detected. As shown in Fig. 5b1, two more isotope clusters with high abundance were found in the isotope clusters of C$_{17}$H$_{30}$Cl$_5$COOH, and their element compositions were generated by the loss of H$_2$ and H$_4$ compared to C$_{17}$H$_{30}$Cl$_5$COOH. Similarly, isotope clusters of C$_{17}$H$_{27}$Cl$_6$COOH ($\Omega = 2$) and C$_{17}$H$_{25}$Cl$_6$COOH ($\Omega = 3$) were found together with those of C$_{17}$H$_{29}$Cl$_6$COOH (Fig. 5b2). As elimination reactions can also occur in basic solutions along with the hydrolysis reaction (Ouellette and Rawn, 2018). these acids with unsaturation degrees higher than 1 were likely to be produced through the elimination reaction of the acids generated by hydrolysis of CP(O$_2$)s (ester). For example, the ester of C$_{19}$H$_{32}$Cl$_6$O$_2$ ([M+Cl]$^-$, m/z 539.02034, $\Omega = 1$) could produce the acid of C$_{17}$H$_{29}$Cl$_6$-COOH ([M+Cl]$^-$, m/z 525.00417, $\Omega = 1$) by hydrolysis and then subsequently generate the acid of C$_{17}$H$_{28}$Cl$_5$-COOH (m/z 489.02818, $\Omega = 2$) by elimination of HCl. More acids with various unsaturation degrees were thus produced through the elimination reactions in strong basic solutions. Based on the above
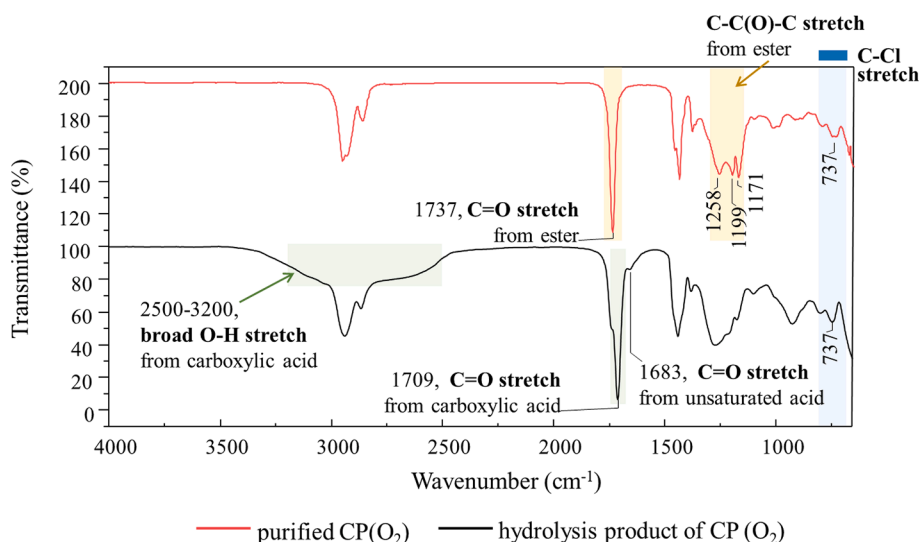

Fig. 4. FT-IR spectra of purified CP(O$_2$)s and their hydrolysis product in the range of 4000–600 cm^{-1}.

Fig. 5. Mass spectra of purified CP(O$_2$)s before (a) and after (b) hydrolysis reaction by direct injection into the chlorine enhanced APCI-Orbitrap MS. Ions with the relationships of reactant-product were marked with the same colors, a1) mass spectra of three CP(O$_2$) congener groups before hydrolysis; b1) and b2) mass spectra showing the resolutions of ions of saturated ($\Omega = 1$) and unsaturated ($\Omega > 1$) chlorinated acids produced during hydrolysis. (For interpretation of the references to color in this figure legend, the reader is referred to the web version of this article.)

results, it can be confirmed that the $CP(O_2)s$ were chlorinated fatty acid methyl esters.

3.4. Environmental occurrences and exposures

Currently, the percentages of known CPs in the commercial mixtures are only 14.1–77.2%, thus the contributions of the newly identified CFAMEs in the mixtures were assessed. In this study, CFAMEs with carbon numbers of 17–19 and 3–11 chlorines were identified, and these congeners have similar carbon numbers compared to the MCCPs and LCCPs. Accordingly, CFAMEs were detected with low mass fractions in CP-42 commercial mixtures, but their mass fractions were relatively high in CP-52 and CP-70 commercial mixtures (1.8–21.3%). In particular, in the CP-52 commercial mixtures from Jiangsu producer, CFAMEs were the predominant component with a high mass fraction of 21.3%. The profiles of CFAMEs were dominated by C_{19}-CFAMEs with 6–8 chlorines, followed by C_{17}-CFAMEs with 5–8 chlorines, and C_{18}-CFAMEs with 5–7 chlorines in the three types of commercial mixtures. As the fatty acid esters with a carbon number of 17 and 19 are widely used in industry (Anneken et al., 2006; Baumann et al., 1988), it is possible that these esters were used in the production of CP commercial mixtures and underwent chlorination to generate the CFAMEs. CFAMEs is a group of industrial products used as plasticizers in PVC and extreme pressure (EP) additive in fluids for abrasive machining together with CPs, and can be synthesized from main ingredients of nature biodiesel (FAMEs) (Guan-Tian et al., 2013; Marinescu et al., 2013). Moreover, some identified CFAMEs, for example $C_{19}Cl_5$-CFAMEs, $C_{19}Cl_4$-CFAMEs, and $C_{18}Cl_4$-CFAMEs, were found in the TSCA inventory lists and REACH Pre-registered substances lists, but the hazard and exposure information of these chemical is not available (ECHA; USEPA).

The newly identified CFAMEs were further determined to be ubiquitous in the environmental samples collected in Shenzhen, a major city of CP production in China. The distinct peaks of $CP(O_2)$ compounds compared to purified $CP(O_2)s$ and CPs detected in the collected samples are shown in Fig. S8. Similar to the CPs commercial mixtures, C_{19}-CFAMEs, C_{17}-CFAMEs, and C_{18}-CFAMEs were the predominant congener groups, suggesting that CFAMEs detected in the environmental samples may have originated from the use and/or production of CP commercial mixtures (Fig. S9, Table S4 and S5,). The total concentrations of CFAMEs were found to be 13 ± 7.7 ng/g in soil samples and 0.773 ± 0.364 ng/m³ in air samples. In food samples, the concentrations of $\sum$CFAMEs were quantified to be 117 ± 84 ng/g ww in meat, 60 ± 21 ng/g ww in egg, 134 ± 127 ng/g ww in fish and shrimp, 41 ± 13 ng/g ww in cereal, 37 ± 25 ng/g ww in vegetables and 160 ± 73 ng/g ww in fruits (Tables S4 ad S5). Chlorinated fatty acids (CFAs) with carbon number of 14, 16, 18 and chlorine number of 1–2 were detected in fish samples from waters contaminated by the nearby pulp industry, and the CFAs were derivatized to CFAMEs for GC analysis (Åkesson-Nilsson, 2003). The present study firstly identified CFAMEs and presented the occurrences of these compounds in environmental samples. The concentrations of newly identified CFAMEs are compared with those of CPs in the environmental samples. The concentration ratios of $\sum$CFAMEs/$\sum$CPs were constantly low in air (0.01–0.54), soil (0.08–0.22) and animal-based foods with high lipid contents (0.01–2.9 for meat, 0.02–0.37 for eggs and 0.12–6.8 for fish&shrimp). In contrast, the $\sum$CFAMEs/$\sum$CPs concentration ratios in plant-based foods with low lipid contents were relatively high in fruits (1.4–12), cereal (0.47–18) and vegetables (0.13–35). These results indicated that CFAMEs were preferentially accumulated in fruits and vegetables compared to the CPs, possibly due to their weaker hydrophobicity caused by polar ester groups.

Moreover, the contributions of different exposure pathways of CFAMEs were estimated according to the dietary habits of local residents (Table S6). As shown in Fig. 6a, the contributions of air respiration and dermal contact with soil were extremely low and 98.1% of CFAME exposures were derived from food consumption, which was similar to
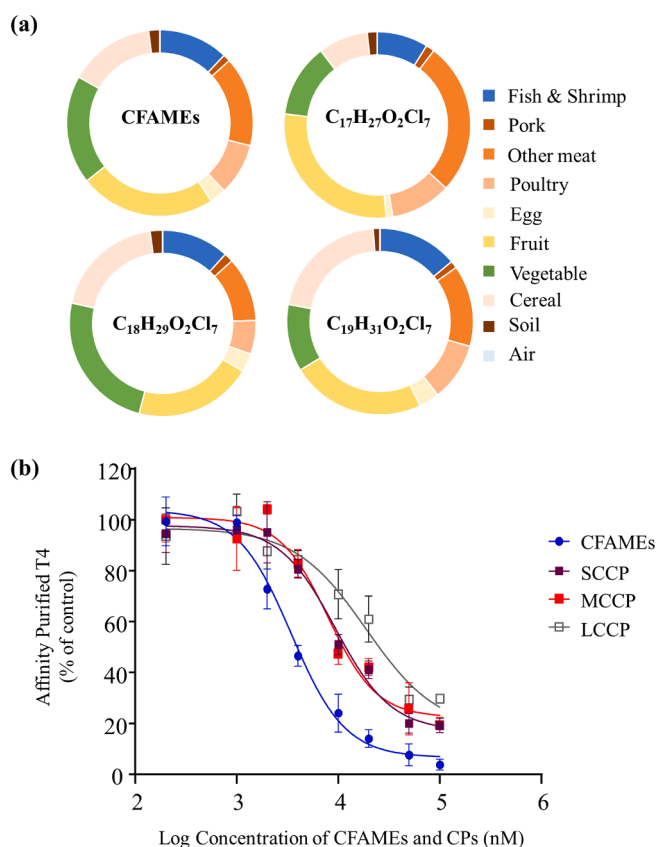
Fig. 6. a) Percentages of contributions to the average daily doses of $\sum$CFAMEs and predominant congener groups ($C_{17}H_{27}O_2Cl_7$, $C_{18}H_{29}O_2Cl_7$, and $C_{19}H_{31}O_2Cl_7$) through multiple exposure routes. b) Competitive binding curves showing T4-TTR interactions with the competitors of CFAMEs and CPs. Results are presented as relative percent of T4 affinity purified by TTR compared to controls (means ± standard deviations). The 50% inhibition of T4-TTR interactions were 3.4 ± 0.3 μM, 9.3 ± 1.1 μM, 8.3 ± 1.3 μM, and 18.7 ± 6.5 μM for CFAMEs, SCCPs, MCCPs, and LCCPs, respectively.

those of CPs (Dong et al., 2020). Of the different types of food, meats had the highest contribution of 25.8%, followed by fruits (23.6%), vegetables (18.8%) and cereal (14.9%). The contributions due to consumption of fruits (23.6%) and vegetables (18.8%) to CFAME exposures were significantly high compared to those of CPs (0.98–1.93% for fruits and 1.16–6.76% for vegetables) (Dong et al., 2020). These results suggested that the newly identified compounds possibly pose a higher risk to populations with high consumption of plant-based foods such as vegetables and fresh fruits (e.g., Asian population). Consistent with the wide environmental occurrence of CFAMEs, these compounds were also detected in the blood of residents in the study areas. The detection frequencies of CFAMEs was as high as 67% in human blood, and the predominant congener groups were C_{17}-CFAMEs, C_{18}-CFAMEs and C_{19}-CFAMEs, of which the chromatograms are shown in Fig. S10. The profiles of the detected CFAMEs were similar to those found in food and air samples (Fig. S9). Blood concentrations of C_{17}-CFAMEs, C_{18}-CFAMEs and C_{19}-CFAMEs were estimated to be 17 ± 26, 17 ± 26 and 19 ± 28 ng/g wet weight, respectively (Table S5). The ubiquitous CFAMEs in humans and the environment indicated that more studies on the toxicity and risk assessments of these new compounds are required.

It is well known that TTR is a transport protein facilitating the placental transfer of hydrophobic pollutants in pregnant women (Chen et al., 2016; Hamers et al., 2020; Wan et al., 2010). Pollutants with potentials to compete with THs for binding sites on TTR would undergo placental transfer and disrupt the homeostasis of THs in development fetus (Darnerud et al., 1996; Hallgren and Darnerud, 2002; Hamers

et al., 2020; Zhao et al., 2017). This study demonstrated the binding affinities of CFAMEs and CPs to TTR by ANSA displacement assay (Fig. 1d). Moreover, affinity purification of chemicals with T4 against TTR showed that CFAMEs and CPs were able to compete with T4 for binding to TTR, and their competitive binding capacities were highest for CFAMEs, followed by SCCPs, MCCPs, and LCCPs (Fig. 6b). The maternal transfer of CPs has been reported (Aamir et al., 2019; Chen et al., 2020; Qiao et al., 2018; Wang et al., 2018), and the newly identified CFAMEs were also detected in human blood in this study. Therefore, CFAMEs had high potentials to undergo TTR-mediated placenta transfer, leading to the adverse effects on TH homeostasis and fetal development.

4. Conclusion

In conclusion, a new group of oxygen-containing CPs were found using a purification method based on the protein affinity of TTR/TR, which successfully identified CFAMEs by a combination of liquid-liquid extraction, hydrolysis, Fourier transform infrared spectrometry and Orbitrap mass spectrometry. CFAMEs with a carbon chain length of 17–19 and 3–11 chlorines were detected with high percentages in the commercial mixtures of CP-52 and CP-70. The identified CFAMEs were found to be ubiquitous in environmental samples. These compounds were also found in human blood mainly through the dietary intake of plant-based foods. CFAMEs had high potentials to undergo TTR-mediated placenta transfer, and more studies on toxicity and potential risks of CFAMEs are required in the future.

CRediT authorship contribution statement

Yibin Sun: Methodology, Investigation, Writing - original draft. **Hongyang Cui:** Methodology, Resources. **Tong Li:** Investigation. **Shu Tao:** Writing - review & editing. **Jianying Hu:** Writing - review & editing. **Yi Wan:** Data curation, Funding acquisition, Project administration, Supervision, Writing - review & editing.

Declaration of Competing Interest

The authors declare that they have no known competing financial interests or personal relationships that could have appeared to influence the work reported in this paper.

Appendix A. Supplementary material

Text, figures, and tables addressing 1) chemicals and reagents, 2) TTR binding experiments, 3) T4 Competitive Binding Test, 4) collection of environmental and human samples, 5) sample preparations, 6) analysis and quantifications of $CP(O_2)$s, 7) details of food samples and human blood collecting participants, 8) chlorinated compounds affinity purified by the TTR protein, 9) concentrations of the detected CFAMEs in air, soil, food and blood samples, 10) exposure parameters, 11) preparation of the His-tagged TR/TTR fusion proteins, 12) locations of commercial CP mixtures manufacturing sites and sample collection sites, 13) PCA score plot of chemical features affinity purified in TTR, TR and control groups, 14) Percentages of extracted CPs by the protein-based affinity purification, 15) mass spectrum patterns of $CP(O_2)$s in the CP commercial mixtures, 16) integrated peak area of FTIR spectra at

characteristic absorptions, 17) chromatograms of detected $CP(O_2)$ ions with CPs ions in environmental samples and $CP(O_2)$s standards, and 18) profiles of detected CFAMEs in environmental samples and human bloods. Supplementary data to this article can be found online at https://doi.org/10.1016/j.envint.2020.106165.

References

Aamir, M., Yin, S., Guo, F., Liu, K., Xu, C., Liu, W., 2019. Congener-specific mother-fetus distribution, placental retention, and transport of C10–13 and C14–17 chlorinated paraffins in pregnant women. Environ. Sci. Technol. 53, 11458–11466.

Åkesson-Nilsson, G., 2003. Isolation of chlorinated fatty acid methyl esters derived from cell-culture medium and from fish lipids by using an aminopropyl solid-phase extraction column. J. Chromatogr. A 996, 173–180.

Anneken, D.J., Both, S., Christoph, R., Fieg, G., Steinberner, U., Westfechtel, A., 2006. Fatty Acids. Ullmann's Encyclopedia of Industrial Chemistry.

Ballesteros-Gomez, A., Rubio, S., 2011. Recent advances in environmental analysis. Anal. Chem. 83, 4579–4613.

Baumann, H., Bühler, M., Fochem, H., Hirsinger, F., Zoebelein, H., Falbe, J., 1988. Natural fats and oils—renewable raw materials for the chemical industry. Angew. Chem. Int. Ed. 27, 41–62.

Bezchlebova, J., Černohlávková, J., Kobetičová, K., Lana, J., Sochová, I., Hofman, J., 2007. Effects of short-chain chlorinated paraffins on soil organisms. Ecotoxicol. Environ. Saf. 67, 206–211.

Birtley, R.D.N., Conning, D.M., Daniel, J.W., Ferguson, D.M., Longstaff, E., Swan, A.A.B., 1980. The toxicological effects of chlorinated paraffins in mammals. Toxicol. Appl. Pharmacol. 54, 514–525.

Bogdal, C., Alsberg, T., Diefenbacher, P.S., MacLeod, M., Berger, U., 2015. Fast quantification of chlorinated paraffins in environmental samples by direct injection high-resolution mass spectrometry with pattern deconvolution. Anal. Chem. 87, 2852–2860.

Brack, W., 2003. Effect-directed analysis: a promising tool for the identification of organic toxicants in complex mixtures? Anal. Bioanal. Chem. 377, 397–407.

Bucher, J.R., Alison, R.H., Montgomery, C.A., Huff, J., Haseman, J.K., Farnell, D., Thompson, R., Prejean, J.D., 1987. Comparative toxicity and carcinogenicity of two chlorinated paraffins in F344/N rats and B6C3F1 mice. Toxicol. Sci. 9, 454–468.

Burgess, R.M., Berry, W.J., Mount, D.R., Di Toro, D.M., 2013a. Mechanistic sediment quality guidelines based on contaminant bioavailability: equilibrium partitioning sediment benchmarks. Environ. Toxicol. Chem. 32, 102–114.

Burgess, R.M., Ho, K.T., Brack, W., Lamoree, M., 2013b. Effects-directed analysis (EDA) and toxicity identification evaluation (TIE): complementary but different approaches for diagnosing causes of environmental toxicity. Environ. Toxicol. Chem. 32, 1935–1945.

Bytingsvik, J., Simon, E., Leonards, P.E.G., Lamoree, M., Lie, E., Aars, J., Derocher, A.E., Wiig, Ø., Jenssen, B.M., Hamers, T., 2013. Transthyretin-binding activity of contaminants in blood from polar bear (Ursus maritimus) cubs. Environ. Sci. Technol. 47, 4778–4786.

Chen, H., Zhou, W., Lam, J.C.W., Ge, J., Li, J., Zeng, L., 2020. Blood partitioning and whole-blood-based maternal transfer assessment of chlorinated paraffins in mother-infant pairs from South China. Environ. Int. 142, 105871.

Chen, M., Fan, Z., Zhao, F., Gao, F., Mu, D., Zhou, Y., Shen, H., Hu, J., 2016. Occurrence and maternal transfer of chlorinated bisphenol A and nonylphenol in pregnant women and their matching embryos. Environ. Sci. Technol. 50, 970–977.

Cooley, H., Fisk, A., Wiens, S., Tomy, G., Evans, R., Muir, D., 2001. Examination of the behavior and liver and thyroid histology of juvenile rainbow trout (Oncorhynchus mykiss) exposed to high dietary concentrations of C10-, C11-, C12-and C14-polychlorinated n-alkanes. Aquat. Toxicol. 54, 81–99.

Darnerud, P.O., Morse, D., Klasson-Wehler, E., Brouwer, A., 1996. Binding of a 3,3′,4,4′-tetrachlorobiphenyl (CB-77) metabolite to fetal transthyretin and effects on fetal thyroid hormone levels in mice. Toxicology 106, 105–114.

de Boer, C., 2010. Chlorinated paraffins ed~eds. Springer.

Dong, Z., Li, T., Wan, Y., Sun, Y., Hu, J., 2020. Physiologically based pharmacokinetic modeling for chlorinated paraffins in rats and humans: importance of biliary excretion. Environ. Sci. Technol. 54, 938–946.

ECHA. Pre-registered substances. can be founded under https://echa.europa.eu/information-on-chemicals/pre-registered-substances.

Feo, M., Eljarrat, E., Barcelo, D., 2009. Occurrence, fate and analysis of polychlorinated n-alkanes in the environment. Trac-Trends Anal. Chem. 28, 778–791.

Gao, Y., Zhang, H., Su, F., Tian, Y., Chen, J., 2012. Environmental occurrence and distribution of short chain chlorinated paraffins in sediments and soils from the Liaohe river basin, P.R. China. Environ. Sci. Technol. 46, 3771–3778.

Glüge, J., Wang, Z., Bogdal, C., Scheringer, M., Hungerbühler, K., 2016a. Global production, use, and emission volumes of short-chain chlorinated paraffins – A minimum scenario. Sci. Total Environ. 573, 1132–1146.

Glüge, J., Wang, Z., Bogdal, C., Scheringer, M., Hungerbühler, K., 2016b. Global production, use, and emission volumes of short-chain chlorinated paraffins–A minimum scenario. Sci. Total Environ. 573, 1132–1146.

Gong, Y., Zhang, H., Geng, N., Xing, L., Fan, J., Luo, Y., Song, X., Ren, X., Wang, F., Chen, J., 2018. Short-chain chlorinated paraffins (SCCPs) induced thyroid disruption by enhancement of hepatic thyroid hormone influx and degradation in male Sprague Dawley rats. Sci. Total Environ. 625, 657–666.

Guan-Tian, M.O., Huang, Z.P., Xu, W.U., 2013. Synthesis and Application of Fatty Acid Methyl Ester Chloride. Guangzhou Chemical Industry.

Hahladakis, J.N., Velis, C.A., Weber, R., Iacovidou, E., Purnell, P., 2018. An overview of chemical additives present in plastics: migration, release, fate and environmental impact during their use, disposal and recycling. J. Hazard. Mater. 344, 179–199.

Hallgren, S., Darnerud, P.O., 2002. Polybrominated diphenyl ethers (PBDEs), polychlorinated biphenyls (PCBs) and chlorinated paraffins (CPs) in rats—testing interactions and mechanisms for thyroid hormone effects. Toxicology 177, 227–243.

Hamers, T., Kortenkamp, A., Scholze, M., Molenaar, D., Cenijn, P.H., Weiss, J.M., 2020. Transthyretin-binding activity of complex mixtures representing the composition of thyroid-hormone disrupting contaminants in house dust and human serum. Environ. Health Perspect. 128, 017015.

Harada, K.H., Takasuga, T., Hitomi, T., Wang, P., Matsukami, H., Koizumi, A., 2011. Dietary exposure to short-chain chlorinated paraffins has increased in Beijing, China. Environ. Sci. Technol. 45, 7019–7027.

Henschler, D., 1994. Toxicity of chlorinated organic compounds: effects of the introduction of chlorine in organic molecules. Angew. Chem. Int. Ed. 33, 1920–1935.

Houde, M., Muir, D.C., Tomy, G.T., Whittle, D.M., Teixeira, C., Moore, S., 2008. Bioaccumulation and trophic magnification of short-and medium-chain chlorinated paraffins in food webs from Lake Ontario and Lake Michigan. Environ. Sci. Technol. 42, 3893–3899.

Hu, W., Jia, Y., Kang, Q., Peng, H., Ma, H., Zhang, S., Hiromori, Y., Kimura, T., Nakanishi, T., Zheng, L., 2019. Screening of house dust from Chinese homes for chemicals with liver X receptors binding activities and characterization of atherosclerotic activity using an in vitro macrophage cell line and ApoE−/− Mice. Environ. Health Perspect. 127, 117003.

Ishihara, A., Sawatsubashi, S., Yamauchi, K., 2003. Endocrine disrupting chemicals: interference of thyroid hormone binding to transthyretins and to thyroid hormone receptors. Mol. Cell. Endocrinol. 199, 105–117.

Landers, K.A., Mortimer, R.H., Richard, K., 2013. Transthyretin and the human placenta. Placenta 34, 513–517.

Li, H., Zhang, J., You, J., 2018a. Diagnosis of complex mixture toxicity in sediments: Application of toxicity identification evaluation (TIE) and effect-directed analysis (EDA). Environ. Pollut. 237, 944–954.

Li, T., Gao, S., Ben, Y., Zhang, H., Kang, Q., Wan, Y., 2018b. Screening of chlorinated paraffins and unsaturated analogues in commercial mixtures: confirmation of their occurrences in the atmosphere. Environ. Sci. Technol. 52, 1862–1870.

Liu, L., Li, Y., Coelhan, M., Chan, H.M., Ma, W., Liu, L., 2016. Relative developmental toxicity of short-chain chlorinated paraffins in Zebrafish (Danio rerio) embryos. Environ. Pollut. 219, 1122–1130.

Marinescu, I.D., Rowe, W.B., Dimitrov, B., Ohmori, H., 2013. 15 - Process fluids for abrasive machining. In: Marinescu, I.D., Rowe, W.B., Dimitrov, B., Ohmori, H. (Eds.), Tribology of Abrasive Machining Processes, second ed. William Andrew Publishing, Oxford.

Mondal, S., Raja, K., Schweizer, U., Mugesh, G., 2016. Chemistry and biology in the biosynthesis and action of thyroid hormones. Angew. Chem. Int. Ed. 55, 7606–7630.

Montaño, M., Cocco, E., Guignard, C., Marsh, G., Hoffmann, L., Bergman, Å., Gutleb, A. C., Murk, A.J., 2012. New approaches to assess the transthyretin binding capacity of bioactivated thyroid hormone disruptors. Toxicol. Sci. 130, 94–105.

Muir, D., Stern, G., Tomy, G., 2000. Chlorinated paraffins, vol. 3. Springer, Anthropogenic Compounds Part K.

Ortiga-Carvalho, T.M., Sidhaye, A.R., Wondisford, F.E., 2014. Thyroid hormone receptors and resistance to thyroid hormone disorders. Nat. Rev. Endocrinol. 10, 582–591.

Ouellette, R.J., Rawn, J.D., 2018. 10 - Nucleophilic substitution and elimination reactions. In: Ouellette, R.J., Rawn, J.D. (Eds.), Organic Chemistry, second ed. Academic Press.

Park, J.-S., Bergman, Å., Linderholm, L., Athanasiadou, M., Kocan, A., Petrik, J., Drobna, B., Trnovec, T., Charles, M.J., Hertz-Picciotto, I., 2008. Placental transfer of polychlorinated biphenyls, their hydroxylated metabolites and pentachlorophenol in pregnant women from eastern Slovakia. Chemosphere 70, 1676–1684.

Patel, J., Landers, K., Li, H., Mortimer, R.H., Richard, K., 2011. Delivery of maternal thyroid hormones to the fetus. Trends Endocrinol. Metab. 22, 164–170.

Paul-Friedman, K., Martin, M., Crofton, K.M., Hsu, C.-W., Sakamuru, S., Zhao, J., Xia, M., Huang, R., Stavreva, D.A., Soni, V., Varticovski, L., Raziuddin, R., Hager, G.L., Houck, K.A., 2019. Limited chemical structural diversity found to modulate thyroid hormone receptor in the Tox21 chemical library. Environ. Health Perspect. 127, 097009.

Peng, H., Sun, J., Alharbi, H.A., Jones, P.D., Giesy, J.P., Wiseman, S., 2016. Peroxisome proliferator-activated receptor γ is a sensitive target for oil sands process-affected water: effects on adipogenesis and identification of ligands. Environ. Sci. Technol. 50, 7816–7824.

Petrovic, M., Eljarrat, E., de Alda, M.J.L., Barcelo, D., 2004. Endocrine disrupting compounds and other emerging contaminants in the environment: A survey on new monitoring strategies and occurrence data. Anal. Bioanal. Chem. 378, 549–562.

Pleasure, J.R., Pleasure, D., Pleasure, S.J. 2017. 133 - Trophic factor, nutritional, and hormonal regulation of brain development. In: Polin R.A., Abman S.H., Rowitch D. H., Benitz W.E., Fox W.W. (eds.), Fetal and Neonatal Physiology, fifth ed. Elsevier.

Poon, R., Lecavalier, P., Chan, P., Viau, C., Håkansson, H., Chu, I., Valli, V., 1995. Subchronic toxicity of a medium-chain chlorinated paraffin in the rat. J. Appl. Toxicol. 15, 455–463.

Qiao, L., Gao, L., Zheng, M., Xia, D., Li, J., Zhang, L., Wu, Y., Wang, R., Cui, L., Xu, C., 2018. Mass fractions, congener group patterns, and placental transfer of short- and medium-chain chlorinated paraffins in paired maternal and cord serum. Environ. Sci. Technol. 52, 10097–10103.

Ren, X., Geng, N., Zhang, H., Wang, F., Gong, Y., Song, X., Luo, Y., Zhang, B., Chen, J., 2019. Comparing the disrupting effects of short-, medium- and long-chain

chlorinated Paraffins on cell viability and metabolism. Sci. Total Environ. 685, 297–307.

Ren, X., Zhang, H., Geng, N., Xing, L., Zhao, Y., Wang, F., Chen, J., 2018. Developmental and metabolic responses of zebrafish (Danio rerio) embryos and larvae to short-chain chlorinated paraffins (SCCPs) exposure. Sci. Total Environ. 622, 214–221.

Schinkel, L., Lehner, S., Heeb, N.V., Marchand, P., Cariou, R., McNeill, K., Bogdal, C., 2018. Dealing with strong mass interferences of chlorinated paraffins and their transformation products: An analytical guide. Trac-Trends Anal. Chem. 106, 116–124.

Simon, E., Lamoree, M.H., Hamers, T., de Boer, J., 2015. Challenges in effect-directed analysis with a focus on biological samples. Trac-Trends Anal. Chem. 67, 179–191.

Tang, E., Yao, L., 2005. Industry status of chlorinated paraffin and its development trends. China Chlor-Alkali. 2, 1–3.

Tomy, G., Stern, G., Lockhart, W., Muir, D., 1999. Occurrence of C10–C13 polychlorinated n-alkanes in Canadian midlatitude and arctic lake sediments. Environ. Sci. Technol. 33, 2858–2863.

Tomy, G.T., Stern, G.A., Muir, D.C.G., Fisk, A.T., Cymbalisty, C.D., Westmore, J.B., 1997. Quantifying C10–C13 polychloroalkanes in environmental samples by high-resolution gas chromatography/electron capture negative ion high-resolution mass spectrometry. Anal. Chem. 69, 2762–2771.

Ucán-Marin, F., Arukwe, A., Mortensen, A.S., Gabrielsen, G.W., Letcher, R.J., 2010. Recombinant albumin and transthyretin transport proteins from two gull species and human: chlorinated and brominated contaminant binding and thyroid hormones. Environ. Sci. Technol. 44, 497–504.

UNEP, 2017. Report of the Conference of the Parties to the Stockholm Convention on Persistent Organic Pollutants on the Work of its Eighth Meeting.

USEPA. TSCA Chemical Substance Inventory. can be founded under https://www.epa.gov/tsca-inventory.

USEPA, 2015. Standard Review Risk Assessment on Medium-chain and Long-chain Chlorinated paraffin PMN submissions by Dover Chemical. Can be found under https://www.epa.gov/sites/production/files/2015-12/documents/dover_-_standard_review_risk_assessment_p-12-0282-0284_docket_0.pdf.

van Mourik, L.M., Gaus, C., Leonards, P.E.G., de Boer, J., 2016. Chlorinated paraffins in the environment: A review on their production, fate, levels and trends between 2010 and 2015. Chemosphere 155, 415–428.

van Mourik, L.M., Leonards, P.E., Gaus, C., de Boer, J., 2015. Recent developments in capabilities for analysing chlorinated paraffins in environmental matrices: a review. Chemosphere 136, 259–272.

Volkov, L.I., Kim-Han, J.S., Saunders, L.M., Poria, D., Hughes, A.E.O., Kefalov, V.J., Parichy, D.M., Corbo, J.C., 2020. Thyroid hormone receptors mediate two distinct mechanisms of long-wavelength vision. Proc. Natl. Acad. Sci. 117, 15262.

Wan, Y., Choi, K., Kim, S., Ji, K., Chang, H., Wiseman, S., Jones, P.D., Khim, J.S., Park, S., Park, J., Lam, M.H.W., Giesy, J.P., 2010. Hydroxylated polybrominated diphenyl ethers and bisphenol A in pregnant women and their matching fetuses: placental transfer and potential risks. Environ. Sci. Technol. 44, 5233–5239.

Wang, X., Zhu, J., Kong, B., He, B., Wei, L., Jin, Y., Shan, Y., Wang, W., Pan, C., Fu, Z., 2019a. C9–13 chlorinated paraffins cause immunomodulatory effects in adult C57BL/6 mice. Sci. Total Environ. 675, 110–121.

Wang, X., Zhu, J., Xue, Z., Jin, X., Jin, Y., Fu, Z., 2019b. The environmental distribution and toxicity of short-chain chlorinated paraffins and underlying mechanisms: Implications for further toxicological investigation. Sci. Total Environ. 695, 133834.

Wang, Y., Gao, W., Wang, Y., Jiang, G., 2018. Distribution and pattern profiles of chlorinated paraffins in human placenta of Henan province. China. Environ. Sci. Technol. Lett. 5, 9–13.

Wang, Y., Li, J., Cheng, Z., Li, Q., Pan, X., Zhang, R., Liu, D., Luo, C., Liu, X., Katsoyiannis, A., 2013. Short-and medium-chain chlorinated paraffins in air and soil of subtropical terrestrial environment in the Pearl River Delta, South China: distribution, composition, atmospheric deposition fluxes, and environmental fate. Environ. Sci. Technol. 47, 2679–2687.

Wei, G.-L., Liang, X.-L., Li, D.-Q., Zhuo, M.-N., Zhang, S.-Y., Huang, Q.-X., Liao, Y.-S., Xie, Z.-Y., Guo, T.-L., Yuan, Z.-J., 2016. Occurrence, fate and ecological risk of chlorinated paraffins in Asia: A review. Environ. Int. 92–93, 373–387.

Weiss, J.M., Andersson, P.L., Lamoree, M.H., Leonards, P.E., van Leeuwen, S.P., Hamers, T., 2009. Competitive binding of poly- and perfluorinated compounds to the thyroid hormone transport protein transthyretin. Toxicol. Sci. 109, 206–216.

Wyatt, I., Coutss, C., Elcombe, C., 1993. The effect of chlorinated paraffins on hepatic enzymes and thyroid hormones. Toxicology 77, 81–90.

Xu, J., Gao, Y., Zhang, H., Zhan, F., Chen, J., 2016. Dispersion of short- and medium-chain chlorinated paraffins (CPs) from a CP production plant to the surrounding surface soils and coniferous leaves. Environ. Sci. Technol. 50, 12759–12766.

Yang, L., Li, J., Lai, J., Luan, H., Cai, Z., Wang, Y., Zhao, Y., Wu, Y., 2016. Placental transfer of perfluoroalkyl substances and associations with thyroid hormones: Beijing prenatal exposure study. Sci. Rep. 6, 21699–21699.

Yuan, B., Wang, T., Zhu, N., Zhang, K., Zeng, L., Fu, J., Wang, Y., Jiang, G., 2012. Short chain chlorinated paraffins in mollusks from coastal waters in the Chinese Bohai Sea. Environ. Sci. Technol. 46, 6489–6496.

Zeng, L., Chen, R., Zhao, Z., Wang, T., Gao, Y., Li, A., Wang, Y., Jiang, G., Sun, L., 2013. Spatial distributions and deposition chronology of short chain chlorinated paraffins in marine sediments across the Chinese Bohai and Yellow Seas. Environ. Sci. Technol. 47, 11449–11456.

Zeng, L., Wang, T., Wang, P., Liu, Q., Han, S., Yuan, B., Zhu, N., Wang, Y., Jiang, G., 2011. Distribution and trophic transfer of short-chain chlorinated paraffins in an aquatic ecosystem receiving effluents from a sewage treatment plant. Environ. Sci. Technol. 45, 5529–5535.

Zhang, Q., Wang, J., Zhu, J., Liu, J., Zhang, J., Zhao, M., 2016. Assessment of the endocrine-disrupting effects of short-chain chlorinated paraffins in in vitro models. Environ. Int. 94, 43–50.

Zhao, F., Chen, M., Gao, F., Shen, H., Hu, J., 2017. Organophosphorus flame retardants in pregnant women and their transfer to chorionic villi. Environ. Sci. Technol. 51, 6489–6497.

Ziegler, S., Pries, V., Hedberg, C., Waldmann, H., 2013. Target identification for small bioactive molecules: finding the needle in the haystack. Angew. Chem. Int. Ed. 52, 2744–2792.